Gigantic Plasmon Resonance Effects on Magneto-Optical Activity of Molecularly-Thin Ferromagnets near Gold Surface

Minoru Osada,[1,2,] Natália Hajduková,[1,3] Kosho Akatsuka,[1] Satoshi Yoguchi,[1] and Takayoshi Sasaki[1,2]*

[1]*International Center for Materials Nanoarchitectonics (MANA), National Institute for Materials Science (NIMS), Tsukuba, Ibaraki 305-0044, Japan*

[2]*CREST, Japan Science and Technology Agency, Kawaguchi, Saitama 332-0012, Japan*

[3]*Institute of Physics, Faculty of Mathematics and Physics, Charles University, Prague, 121 16 Czech Republic*

[*]Corresponding author: tel. + 81 29 860 4352, fax + 81 29 854 9061,
e-mail: osada.minoru@nims.go.jp

Abstract

We report on a new magneto-plasomonic material consisting of 1-nm thick ferromagnetic nanosheets and Au nanoparticles. The magneto-optical (MO) Kerr spectra of $Ti_{0.8}Co_{0.2}O_2$ nanosheets near Au surfaces show a gigantic MO response (~10^6 deg/cm) in the visible wavelength region (380−600 nm), not present in $Ti_{0.8}Co_{0.2}O_2$ nanosheets on a bare glass substrate. The observed peaks correspond to intrinsic $d-d^*$ electronic transitions in $Ti_{0.8}Co_{0.2}O_2$ nanosheets and is consistent with the near-field enhancement of the MO response resulting from the spectral overlap of the surface-plasmon-resonace (SPR) in the Au surface with the electronic transition in $Ti_{0.8}Co_{0.2}O_2$. Similar SPR effects are also achieved in ferromagnetic nanosheet/Au with different compositions and with different separation distances (< 5 nm). This demonstration of SPR-enhanced magneto-optics in the ferromagnetic/plasmonic nanosystem may enable design of nanoarchitectures for miniaturized high-performance MO devices and for remote sensing and imaging of magnetic fields.

Keywords: ferromagnetic nanosheet, surface plasmon resonance, magneto-optical effect, Langmuir-Blodgett deposition, layer-by-layer assembly

Surface plasmon is a coupled mode of electromagnetic waves and collective oscillations of free electrons in metallic nanostructures, which is accompanied by an evanescent near field.[1] Manipulating the surface plasmon in nanostructured materials are now central problems of the growing field of plasmonics;[2,3] in particular, enhancing the surface plasmon, a phenomenon termed as surface plasmon resonance (SPR), is of importance for the basis of surface-enhanced Raman scattering (SERS),[4,5] biosensing,[6] electromagnetic waveguide,[7,8] and subwavelength lithography.[9] The overwhelming majority of current SPR studies has focused on Au or Ag nanoparticles because these metals have suitable optical constants for applications with visible-wavelength lights.[10] However, once the size, morphology, and composition of a nanostructure have been fixed, it is difficult to change or control the SPR properties by external means, which would be desirable for the development of active plasmonic nanodevices.

Magnetic materials combined with the plasmonic structure are appealing for new applications in plasmonics because they open up the possibility of using external magnetic fields in plasmonic devices.[11] In such nanostructures, their optical properties change markedly even with a weak magnetic field. A strong enhancement of the magneto-optical (MO) properties is also possible due to the strong electro-magnetic field associated with the localized SPR. Several attempts to develop these kinds of nanostructures have been carried out by forming continuous thin films of Au/Co/Au multilayers.[12,13] More recently, the

enhancement of the MO response due to the localized SPR effects has also been found in magnetic films integrated with Au nanoparticles,[14] Au/Co/Au nanosandwich structures,[15] and core-shell nanoparticles.[16] In these nanostructures, however, the enhancement factors of the MO response lie in the range of 2 − 3, which is much smaller than other SPR phenomena like SERS (of 10^5 − 10^6). Here, we show a new platform for magneto-plasmonic effects, where a gigantic SPR effect (of > 10^3) on the MO activity occurs when 1-nm thick ferromagnetic nanosheets ($Ti_{0.8}Co_{0.2}O_2$) are placed in the proximity to Au surfaces.

Ferromagnetic nanosheet is a new class of ferromagnet based on two-dimensional (2D) nanosheet derived from layered titanate by exfoliation.[17,18] 2D nanosheets, which possess a molecular dimension (~ 1 nm) in the thickness and have a micrometer length in the plane (Figure 1a), are emerging as an important ferromagnetic nanomaterial because of their room-temperature ferromagnetism (~1.4 μ_B/Co)[17] and robust MO response (~10^4 deg/cm) in the ultraviolet wavelength.[18] Due to their highly 2D anisotropy and colloidal nature, nanosheets can be organized into various assemblies such as multilayers, superlattices, and heterostructures, through which we can control/design the cooperative interaction between organized components. These features make ferromagnetic nanosheet an ideal system for studying magneto-plasmonic effects, *e.g.*, by forming nanofilms of ferromagnetic nanosheets onto Au nanoparticles. In this way, we can control the spatial localization of the electro-magnetic field in 1-nm thick ferromagnetic nanosheets, promoting the near-field enhancement of the MO process. Here, we demonstrate that, in such a magneto-plasmonic nanostructure, the strong confinement of the electro-magnetic field in 1-nm thick ferromagnetic nanosheets causes a gigantic enhancement (~10^3) of the MO properties. Moreover, the MO properties are strongly linked to the SPR spectrum, which can be tuned by modifying of the composition of ferromagnetic nanosheets.

The nanostructured films composed of 1-nm thick ferromagnetic monolayer on Au nanoparticles were fabricated by a self-assembly process (Figure 1b). Au colloidal nanoparticles, prepared by chemical reduction of $HAuCl_4$ using sodium borohydride and sodium citrate, were immobilized to a glass substrate.[19] Au nanoparticles formed are nearly monodispersed with the average diameter of ~50 nm. A colloidal suspension of ferromagnetic nanosheet ($Ti_{0.8}Co_{0.2}O_2$) was used to deposit ferromagnetic monolayer by Langmuir-Blodgett technique[20] on the Au-coated substrates. X-ray photoelectron spectroscopy was used to identify the composition of the assembled films (Figure 1c). The film of $Ti_{0.8}Co_{0.2}O_2$/Au exhibited many peaks, which can be assigned to Ti, Co, O, C, and N from film components as well as Au and Si from the substrate.

The plasmonic and MO properties were analyzed by UV-visible spectroscopy and MO Kerr spectroscopy, respectively. The MO Kerr effect consisted of a change in the reflectivity of the magnetic material when a magnetic field was applied. In particular, we employed a polar Kerr configuration (Figure 2a) in which the magnetic field was perpendicular to the films. In this configuration, the light reflected by the magnetized sample was subject to a rotation of the polarization plane and a change in ellipicity state with respect to the incident linearly polarized light.[21] The main data were obtained from the nanostructures composed of ferromagnetic $Ti_{0.8}Co_{0.2}O_2$ nanosheet on Au nanoparticles ($Ti_{0.8}Co_{0.2}O_2$/Au). Complimentary data were obtained by another ferromagnetic nanosheet ($Ti_{0.75}Co_{0.15}Fe_{0.1}O_2$).[22]

Figure 2b shows extinction spectra for monolayer films of $Ti_{0.8}Co_{0.2}O_2$ nanosheet deposited on Au-coated and bare glass substrates. The monolayer $Ti_{0.8}Co_{0.2}O_2$ film without Au does not show any strong absorption in the visible region. In $Ti_{0.8}Co_{0.2}O_2$/Au, on the contrary, a visible absorption band develops at ~530 nm, which can be attributed to the localized SPR of the Au nanoparticles. A characteristic color of the SPR is also seen in the photograph (the inset of Figure 2b).

In Figure 2c, we display magnetic circular dichroism (MCD) spectra for the same films as Figure 2b. The spectrum of a 10-layered $Ti_{0.8}Co_{0.2}O_2$ film on a bare glass substrate is also included for a reference. MCD is proportional to $\Delta\alpha$, which is the difference between the left-hand and right-hand circular polarization absorption coefficients. The 10-layered $Ti_{0.8}Co_{0.2}O_2$ film without Au shows MCD peaks near the bandgap region (~300 nm) due to the Zeeman splitting of the Co^{2+} 3*d* band,[17,18] whereas no well-resolved feature can be discerned in the monolayer $Ti_{0.8}Co_{0.2}O_2$ film. In $Ti_{0.8}Co_{0.2}O_2$/Au, on the contrary, the

amplification of the MO effect by ~10^3 is observed in the presence of Au; the MCD spectrum shows pronounced features at about 390, 470, and 600 nm, which are not present in $Ti_{0.8}Co_{0.2}O_2$ nanosheets. We also note that the observed MO response is reached to 1.7×10^6 deg/cm, a value being the highest seen so far in MO materials.

The overall signal in the Kerr configuration consists of two contributions. The first is the direct reflection by the nanosheet film and the second contribution comes from the light passing through the film and reflected from the film/Au interface. Because the optical density of the ferromagnetic monolayer is low (< 0.01) in the visible region (Figure 2b), it is reasonable to assume that the second contribution is the major one in the case of $Ti_{0.8}Co_{0.2}O_2$/Au.

The remarkable feature in $Ti_{0.8}Co_{0.2}O_2$/Au is the appearance of sharp MCD peaks, which are indiscernible in $Ti_{0.8}Co_{0.2}O_2$ nanosheets on the bare glass. It is interesting to note that these MCD peaks fall close to the d−d* transitions observed in some compounds containing Co^{2+} in octahedral geometry.[23-26] The origin of the MCD peaks can thus be traced to the electronic structure of $Ti_{0.8}Co_{0.2}O_2$, specifically the crystal-field transitions of the Co^{2+} electrons; the MCD signal at 390 nm may be attributed to the charge transition of O 2p to Co 3d, and the peaks at 470 and 600 nm fall close to the d−d* transitions of Co−Co.[23-26]

These d−d* transitions of the Co^{2+} electrons are in principle both spin and parity-forbidden. Hence, these transitions usually make a small contribution to the electronic absorption and MO response in comparison with the stronger electronic absorption transitions observed in the UV region. However, the strength of dipole-forbidden crystal field transitions can be enhanced when electric-dipole transitions that can be ad-mixed to relieve the parity constraint lie close by in energy. The excitation of localized surface plasmon in our nanostructure provides strong dipoles spectrally and spatially close to the d−d* transitions. These plasmon resonances could lead to an increase in the oscillator strength of the d−d* transitions, allowing this transition to contribute to the MO response.

To check the generality of this idea, we also investigated another ferromagnetic nanosheet ($Ti_{0.75}Co_{0.15}Fe_{0.1}O_2$) on Au nanoparticles (Figure 3). This nanosheet is suitable for this purpose, since large MO responses induced by the d−d* transitions are observed even in the multilayered films on the bare glass.[22] We found that such a magneto-plasmonic effect is not limited to $Ti_{0.8}Co_{0.2}O_2$ nanosheet. As is clearly seen in Figure 3, a similar SPR effect is also observed in $Ti_{0.75}Co_{0.15}Fe_{0.1}O_2$, in which the spectral features are more complicated due to the mixed-valence states with the coexistence of (Co^{2+}/Co^{3+}) and (Fe^{2+}/Fe^{3+}) ions, distinct from $Ti_{0.8}Co_{0.2}O_2$ case. In $Ti_{0.75}Co_{0.15}Fe_{0.1}O_2$, the MCD peaks induced by the d−d* transitions are strongly resonated; strong features at about 510 and 590 nm fairly agree with the d−d* transitions involving Co^{2+} and Fe^{3+}. These MCD peaks thus correspond to an intrinsic electronic transition in ferromagnetic nanosheets and is consistent with a near-field enhancement of MO response resulting from the spectral overlap of the SPR in the Au nanoparticles with the electronic transition in $Ti_{1-x}M_xO_2$ (M =Co, Fe). These results suggest that the MCD peaks in our $Ti_{1-x}M_xO_2$/Au system are a consequence of the close proximity of ferromagnetic nanosheets and the Au surface.

In order to further study the proximity effects, we fabricated hetero-assemblies of $Ti_{0.8}Co_{0.2}O_2$/$(Ti_{0.91}O_2)_n$/Au (Figure 4a) by electrostatic layer-by-layer assembly.[27] Here, the interleaving layer of non-magnetic (dielectric) nanosheet ($Ti_{0.91}O_2$)[28,29] were stacked on the Au-coated substrates before depositing the ferromagnetic nanosheet. In this way, we can control the separation distances between the ferromagnetic monolayer and the Au surface. UV-visible absorption monitored on the bare glass reference indicates the successful buildup of $Ti_{0.8}Co_{0.2}O_2$/$(Ti_{0.91}O_2)_n$ in the designed sequence.

Figure 4b displays the change in MCD spectrum for $Ti_{0.8}Co_{0.2}O_2$/$(Ti_{0.91}O_2)_n$/Au with n = 0, 1, 3, 5. Figure 4c plots the intensity of MCD peak as a function of the separation distance. Here, the separation values are calibrated using the intersheet spacing (1.4 nm) determined by X-ray diffraction. Clearly, the increase of the separation between ferromagnetic nanosheet and Au causes the decrease in the enhancement of the MCD response. There appears to be a sharp decrease in the enhancement with the increase in the separation distance, and the resonant feature is almost suppressed at the separation distance of about 5 nm. This situation is similar to what observed in distance-dependent SERS experiments

where SERS on molecules bound to Au substrates showed a similar decrease of signal with increasing separation between molecules and Au.[30] Thus, our results appear to pertain to the same class of other surface-enhanced phenomena where the spectrum of the scattered light is affected by the SPR in the evanescent near field (< 5 nm). Gigantic MO effects observed here suggest that, by optimizing the noble metal-magnetic nanocrystals configuration, it would be possible to significantly increase the magneto-plasmonic effects in MO devices as well as various SPR phenomena such as SERS, electromagnetic waveguide.

In summary, we have explored a new magneto-plasmonic material consisting of molecularly thin ferromagnetic nanosheet and Au nanoparticles. In $Ti_{0.8}Co_{0.2}O_2$/Au, a gigantic SPR effect (of > 10^3) on the MO activity was obseved when 1-nm thick ferromagnetic nanosheets was placed in the proximity to Au surfaces. Moreover, the MO properties were strongly linked to the SPR spectrum, which can be tuned by modifying of the composition of ferromagnetic nanosheets. We also found a sharp decrease in the enhancement with increasing separation between $Ti_{0.8}Co_{0.2}O$ and Au, a situation being similar to what observed in distance-dependent SERS experiments. This demonstration of SPR-enhanced magneto-optics in the ferromagnetic/plasmonic nanosystem may enable design of nanoarchitectures for miniaturized high-performance MO devices and for remote sensing and imaging of magnetic fields.

Acknowledgments
This work was partly supported by World Premier International Research Center Initiative (WPI Initiative in Materials Nanoarchitectonics), MEXT, CREST, JST, the Industrial Technology Research Grant Program (06A22702d), NEDO, and the Grant-in-Aid for Scientific research (23107533), MEXT, Japan.

Supporting Information Available.
Materials and experimental procedures. This material is available free of charge via the Internet at http://pubs.acs.org.

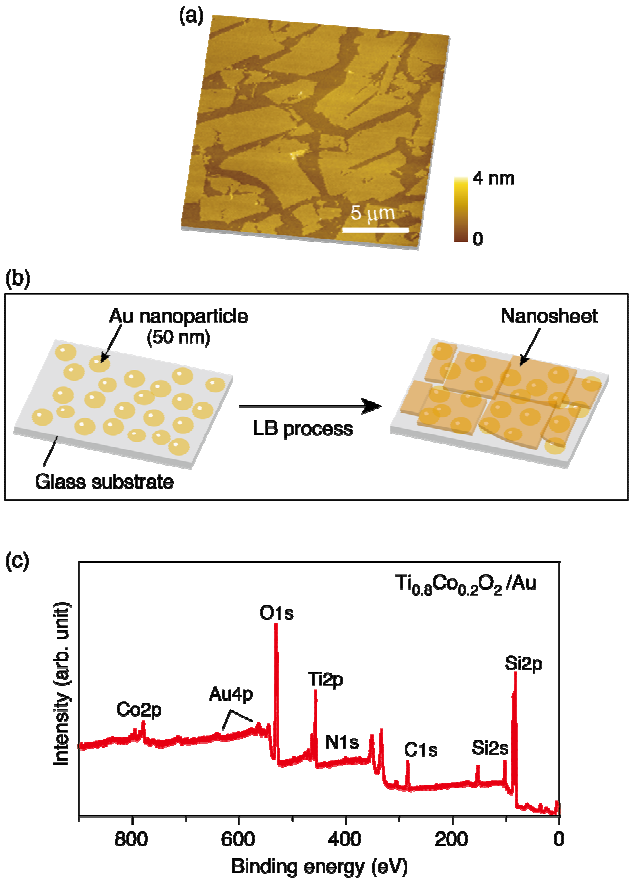

Figure 1. (a) Typical AFM image of $Ti_{0.8}Co_{0.2}O_2$ nanosheets on a Si substrate. (b) Fabrication process for nanostructured film composed of monolayer ferromagnetic nanosheet and Au nanoparticles. (c) Survey XPS spectrum for the nanostructured film composed of $Ti_{0.8}Co_{0.2}O_2$/Au.

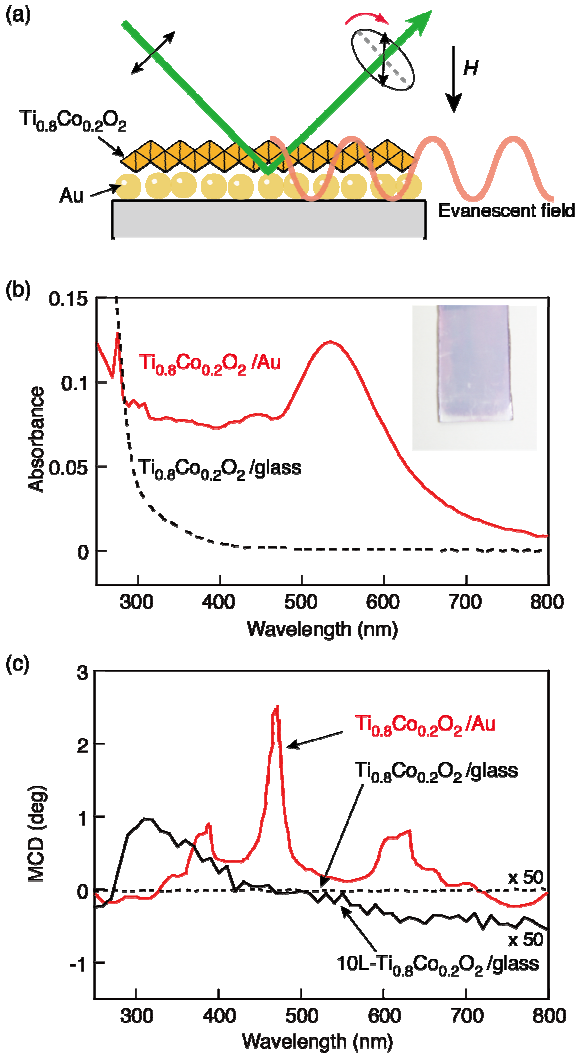

Figure 2. (a) Schematic illustration of our magneto-plasomonic system composed of 1-nm thick ferromagnetic nanosheets and Au nanoparticles. (b) Extinction spectra for the monolayer films of $Ti_{0.8}Co_{0.2}O_2$ nanosheet deposited on Au-coated and bare glass substrates. The inset shows the photograph of $Ti_{0.8}Co_{0.2}O_2$/Au. (c) MCD spectra for the same films as Fig. 2b. The spectrum of a 10 layered $Ti_{0.8}Co_{0.2}O_2$ film on a bare glass substrate is also included for a reference.

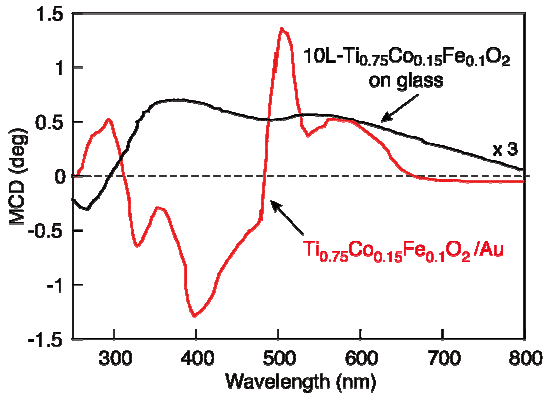

Figure 3. MCD spectra for monolayer $Ti_{0.75}Co_{0.15}Fe_{0.1}O_2$ film on the Au-coated substrate and 10-layered $Ti_{0.75}Co_{0.15}Fe_{0.1}O_2$ film on the bare glass substrate.

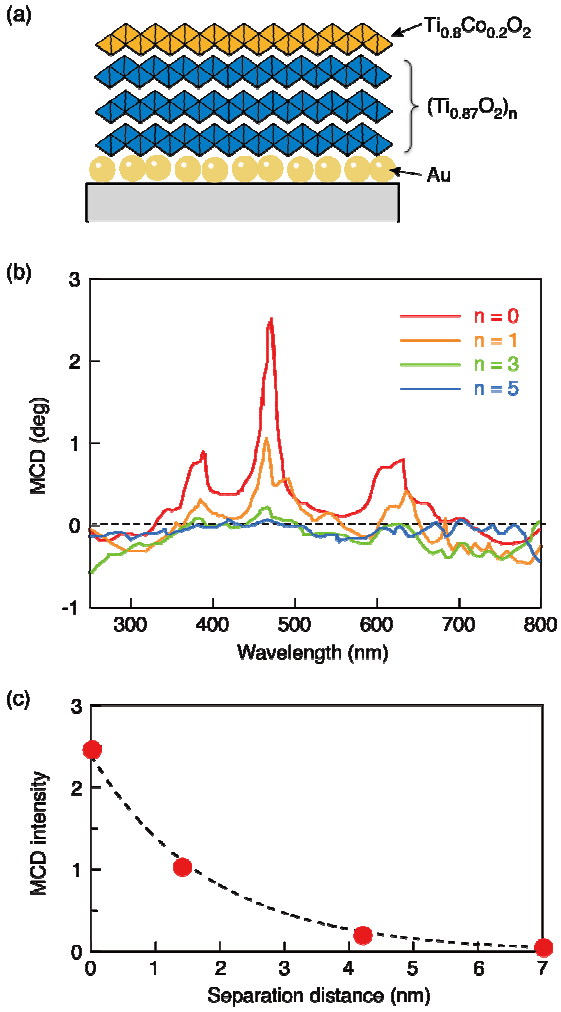

Figure 4. (a) Schematic illustration of hetero-assemblies of $Ti_{0.8}Co_{0.2}O_2/(Ti_{0.91}O_2)_n$/Au. (b) MCD spectra for $Ti_{0.8}Co_{0.2}O_2/(Ti_{0.91}O_2)_n$/Au with n = 0, 1, 3, 5. (c) The change in the MCD peak intensity (at 470 nm) as a function of the separation distance.

References

(1) Ruppin, R. *Electromagnetic Surface Modes*. Boardman, A. D., Ed.; Wiley: Chichester, 1982.

(2) Barnes, W. L.; Dereux, A.; Ebbesen, T. W. *Nature* **2003**, *424*, 824−830.

(3) Ekmel, O. *Science* **2006**, *311*, 189−193.

(4) Nie, S. M.; Emory, S. R. *Science* **1997**, *275*, 1102 –1106.

(5) Xu, H. X.; Bjerneld, E.J.; Käll, M.; Börjesson, L. *Phys. Rev. Lett.* **1999**, *83*, 4357-4360.

(6) Lal, S.; Link, S.; Halas, N. J. *Nat. Photonics*, **2007**, *1*, 641–648.

(7) Maier, S. A.; Brongersma, M. L.; Kik, P. G.; S. Meltzer, S.; Requicha, A. A. G.; Atwater, H. A. *Adv. Mater*. **2001**, *13*, 1501–1505.

(8) Maier, S. A.; Kik, P. G.; Atwater, H. A.; Meltzer, S.; Harel, E.; Koel, B. E.; Requicha, A. A. G. *Nat. Mater*. **2003**, *2*, 229–232.

(9) Luo, X.; Ishihara, T. *Opt. Exp.* **2004**, *12*, 3055–3065.

(10) Xu, H. X.; Aizpurua, J.; Käll, M.; Apell, P. *Phys. Rev. E* **2000**, 62, 4318–4324.

(11) Feil, H.; Haas, C. *Phys. Rev. Lett.* **1987**, *58*, 65–68.

(12) Katayama, T.; Suzuki, Y.; Awano, H.; Nishihara, Y.; Koshizuka, N. *Phys. Rev. Lett.* **1988**, *60*, 1426-1429.

(13) Safarov, V. I.; Kosobukin, V.A.; Hermann, C.; Lampel, G.; Peretti, J.; Marlière, C. *Phys. Rev. Lett*. **1994**, *73*, 3584-3587.

(14) Tomita, S.; Kato, T.; Tsunashima, S.; Iwata, S.; Fujii, M.; Hayashi, S. *Phys. Rev. Lett*. **2006**, *96*, No. 167402.

(15) González-Díaz, J. B.; García-Martín, A.; García-Martín, J. M.; Cebollada, A.; Armelles, G.; Sepúlveda, B.; Alaverdyan, Y.; Käll, M. *Small* **2008**, *4*, 202−205.

(16) Jain, P. K.; Xiao, Y.; Walsworth, R.; Cohen, A. E. *Nano Lett.* **2009**, *9*, 1644−1650.

(17) Osada, M.; Ebina, Y.; Fukuda, K.; Ono, K.; Takada, K.; Yamaura, K.; Takayama-Muromachi, E.; Sasaki, T. *Phys. Rev. B* **2006**, *73*, No. 153301.

(18) Osada, M.; Ebina, Y.; Takada, K.; Sasaki, T. *Adv. Mater*. 2006, *18*, 295−299.

(19) Hajduková, N.; Procházka, M.; Štěpánek, J.; Špírková, M. *Colloids Surf., A* **2007**, *301*, 264−270.

(20) Akatsuka, K.; Haga, M.; Ebina, Y.; Osada, M.; Fukuda, K.; Sasaki, T. *ACS Nano* **2009**, *3*, 1097−1106.

(21) Ando, K. *Magneto-optics of Diluted Magnetic Semiconductors: New Materials and Applications; Magnetio-Optics*. Sugano, S.; N. Kojima, N. Eds.; Springer, Berlin, 2000.

(22) Osada, M.; Itose, M.; Ebina, Y.; Ono, K.; Ueda, S.; Kobayashi, K.; Sasaki, T. *Appl. Phys. Lett.* **2008**, *92*, No. 253110.

(23) Fontijn, W. F. J.; van der Zaag, P. J.; Devillers, M. A. C.; Brabers, V. A. M.; Metselaar, R. *Phys. Rev. B* **1997**, *56*, 5432−5442.

(24) Fontijn, W. F. J.; van der Zaag, P. J.; Feiner, L. F.; Metselaar, R.; Devillers, M. A. C. *J. Appl. Phys.* **1999**, *85*, 5100–5105.

(25) Kim, K. J.; Lee, H. S.; Lee, M. H.; Lee, S. H. *J. Appl. Phys*. **2002**, *91*, 9974–9977.

(26) Liu, Z. P.; Ma, R.; Osada, M.; Iyi, N.; Ebina, Y.; Takada, K.; Sasaki, T. *J. Am. Chem. Soc*. **2006**, *128*, 4872–4880.

(27) Sasaki, T.; Ebina, Y.; Tanaka, T.; Harada, M.; Watanabe, M.; Decher, G. *Chem. Mater*. **2001**, *13*, 4661–4667.

(28) Osada, M.; Ebina, Y.; Funakubo, H.; Yokoyama, S.; Kiguchi, T.; Takada, K.; Sasaki, T. *Adv. Mater*. **2006**, *18*, 1023–1027.

(29) Osada, M.; Sasaki, T. *J. Mater. Chem.* **2009**, *19*, 2503–2511.

(30) Kovacs, G.J.; Loutfy, R. O.; Vincett, P. S.; Jennings, C; Aroca, R. *Langmuir* **1986**, *2*, 689–694.